Proceedings of IDETC/CIE 2005
ASME 2005 International Design Engineering Technical Conferences
& Computers and Information in Engineering Conference
September 24-28, 2005, Long Beach, California USA

DETC2005-85155

DESIGN OF HEAT-REVERSIBLE SNAP JOINTS FOR SPACE FRAME BODIES

Mohammed Shalaby and **Kazuhiro Saitou**[*]
Department of Mechanical Engineering
University of Michigan
Ann Arbor, MI 48109-2125, USA
E-mail:{mshalaby, kazu}@umich.edu

ABSTRACT

This paper presents the design of new joints, heat-reversible snaps, which allow easy, non-destructive, and clean detaching between internal frames and external panels in automotive bodies. It is expected to dramatically reduce the end-of-life environmental impacts of the aluminum space frame bodies, which currently suffer from poor material recyclability. While the assembly process is analogous to normal locator-snap systems, the heat-reversible snaps can be unlocked non-destructively upon heating the panel at a certain location, via the non-uniform thermal deformation of the panel. The optimum number and locations of the locators on the given panel are found based on the equivalent springs that represent the stiffness of the locator. Then, the locations of snaps and heating that ensure unlocking upon heating of the minimum area on the panel are obtained. Finally, a case study on an automotive fender panel assembly is discussed.

INTRODUCTION

Aluminum space frame (Figure 1) is considered as the next generation body structure [1, 2] due to its lightweight, improved rigidity, and design freedom realized by the separation of "bone" and "skin" [3]. They are also environmentally sound since the environmental impact (mainly CO_2 emission) during the use phase of the vehicle is very low due to the improved fuel efficiency (32% of fuel savings) owing to its lightweight (40% lighter than steel body [2]). According to the previous results of life-cycle analyses [1, 4], it is essential to improve the recyclability of aluminum space frame bodies in order to compare with the steel bodies, which currently, have lower energy consumption for production and higher recyclability as a raw material.

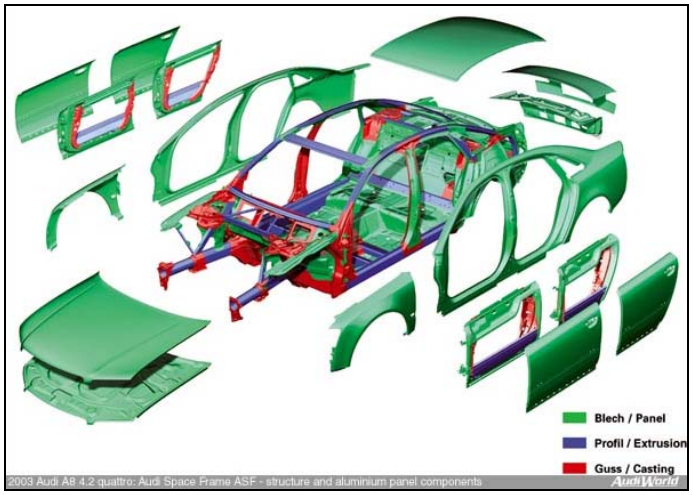

Figure 1: Audi Space Frame [5].

One of the challenges in improving the recyclability of the aluminum space frame body structure is the clean separation of incompatible materials used in various body components, in particular, extruded aluminum structural frames and stamped (or sometimes injection-molded) external panels. In the current aluminum space frame bodies, joining between the internal frames and the external panels is achieved using permanent joints such as self-piercing rivets and resistance spot-welding. These permanent joints can only be detached destructively, inevitably leaving residues of mating materials that prevent the "closed loop" recycling of aluminum alloys. A study conducted by the Aluminum Company of America (ALCOA) [2] predicts that: if the current increasing trend of aluminum use in vehicles continues (which will further boost with the introduction of aluminum space frame bodies), there will be an abundance of unused cast aluminum, unless recycling to the same grade alloy

[*] Corresponding author

("closed loop" recycling) becomes economically feasible. It is essential, therefore, to develop a joining method that allows easy, non-destructive detaching at a desired time.

In this research, the use of heat-actuated reversible snap fits for automotive frame/panel assembly is proposed. While the assembly process is analogous to normal locator-snap systems, the heat-reversible snaps can be unlocked non-destructively upon heating the panel at a certain location, via the non-uniform thermal deformation of the panel. The optimum number and locations of the locators on the given panel are found based on the equivalent springs that represent the stiffness of the locator. Then, the optimum snap and heating locations, which ensure unlocking upon heating of the minimum area on the panel, are obtained. While developed for automotive panel/frame assembly, the design method is generic and can be applied to different areas other than the frame/panel assembly. A case study on an automotive fender panel assembly is discussed.

RELATED WORK

Analysis and Design of Snap Fits

Snap-fit is a preferred joining method for design for disassembly because: no need of extra parts for separation, easily assembled, can be disassemblable, reduces overall product cost and makes the recycling process more economic, and provides clean separation between frame and panel [6 - 8]. Early work on integral attachment design focused on the analysis of particular types of locking features such as cantilever hooks [9], bayonet-fingers [10], compressible hooks [11], *etc*. More recently, Genc *et al.* [12 - 14] discussed a feature-based method to integral attachment design, which classified snap-fit features into three categories: locating features, locking features, and enhancing features. Luscher *et al.* [15] discussed a similar classification based on assembly motions. These works, however, did not address the reversible snap-fit designs that are actuated by thermal deformation.

Design for Disassembly with Reversible Joints

Easy-to-disengage joints can help reducing disassembly efforts, thus making the recycling process economically feasible. Chiodo *et al.* [16 - 19] demonstrated the self-disengaging fastener screws made of a special Shape Memory Polymer (SMP) and compression springs for the eventual disassembly. Masui *et al.* [20] used nichrome wires embedded along the desired boundary of separation, for the active disassembly of CRTs. Although these examples were effective in the particular cases presented, both methods lack generality since they required the use of specialized and costly materials such as SMP.

In our previous work, Li *et al.* [21], used topology optimization to design reversible integral attachments (snap fits) that can be detached by the application of localized heat. A metallic thermal force applicator (TFA), integrated with an engaging plastic part (snap-fit), is heated and the resulting thermal deformation induces the release of the snapped joint, through the transmission of the deformation of TFA to the plastic part. Later, researches utilized the localized heat without TFA, for better deformation characteristics [22, 23]. However, because the unlocking motions of these snap designs rely solely on the local thermal deformations of the snap, this resulted in opening actions that are too small for practical applications. The new heat-reversible snap designs, presented in this paper, overcome this problem, by utilizing the deformation of the panel, whose thermal deformation is much larger than the snaps, as a main driver of the unlocking motion.

HEAT-REVERSIBLE SNAP JOINTS

Design Concept

Figure 2 illustrates the design concept of heat-reversible snap joint. Figure 2 (a) is an internal frame structure with a *catch* (a thin plate with a square hole to which the snap locks into), and Figure 2 (b) is an external panel (backside shown) with locators to hold the frame and a *snap*, a wedge-like feature to lock into the catch. It is essentially a conventional locator-snap system found in literature [24], hence the analogous engaging action is shown in Figure 3. The elasticity of the panel (and to some extent the catch), not the snap and locators, is exploited to enable the snapping action. This allows the locators to be stiff enough to meet the structural requirements of the joints, compared to the elastic cantilever snaps. Similarly, Figure 4 illustrates the disengagement of the panel from the frame. Upon the heat application to the panel (Figure 4 (a)), thermal expansion causes bulging of the panel, which in turn unlocks the snap from the catch (Figure 4 (b)). Then, the panel can be removed from the frame in a reverse manner to the engagement.

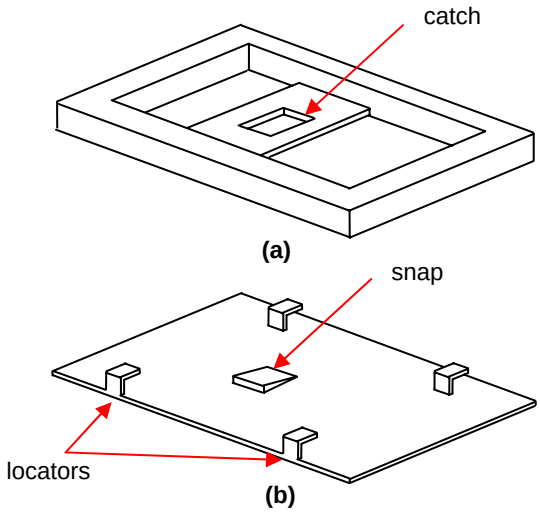

Figure 2: heat-reversible snap joint: (a) frame with a catch and (b) panel with four locators and a snap.

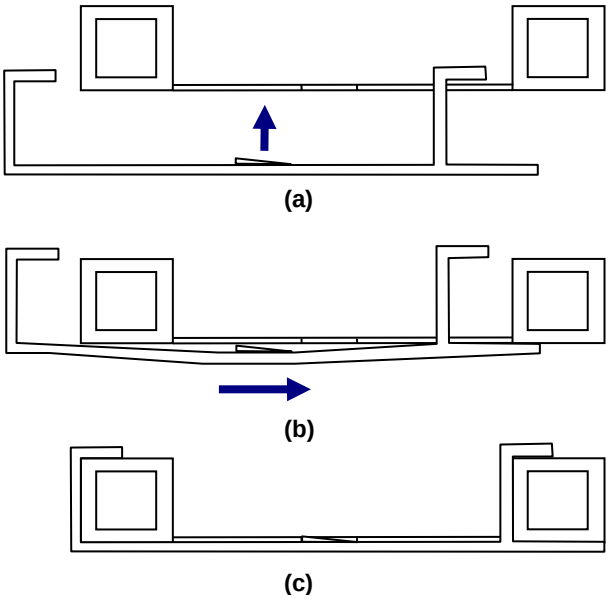

Figure 3: Engagement of heat-reversible snap: (a) push, (b) slide, and (c) lock.

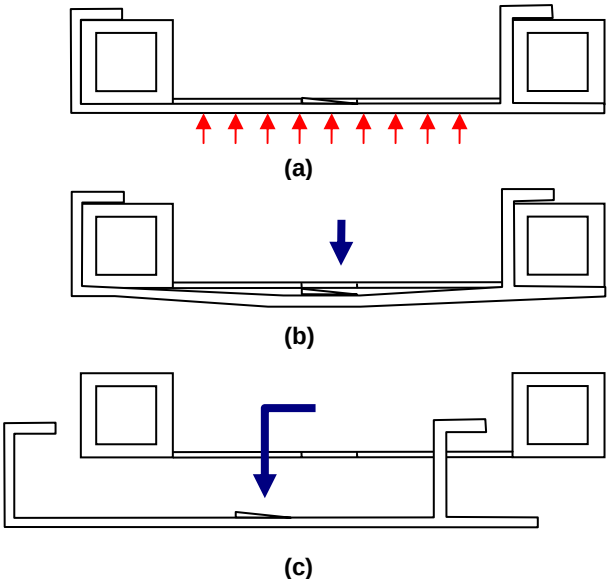

Figure 4: Disengagement of heat-reversible snap: (a) heat, (b) unlock, and (c) slide and remove.

Since the panel deformation is an integral part of the unlocking action, the number and location of the locators and snaps must be carefully designed to meet any structural requirement of the joints while ensuring the unlocking upon heating. Given the panel and frame geometries, the design proceeds in the following two steps:

1. **Locator design:** Find the optimum locations of locators to meet the desired structural properties.
2. **Snap design:** Find the optimum locations of snaps and heating zone for unlocking with minimum heating area.

Although steps 1 and 2 should ideally be addressed simultaneously, doing so would require much computation, since each step involves the optimization using finite element analyses. Considering the primary function of joints is to satisfy their structural requirements, it is placed as the first of the two steps in this paper, which works fine as illustrated in the following case study.

Locator Design

Since several locators are required to securely attach a panel to a frame, their locations on the panel must be determined to meet the structural requirements, such as stiffness and vibration. Through optimization, the minimum number of locators and their locations are determined, which satisfy the constraints on the structural performances evaluated by finite element analyses:

$$\begin{aligned} &\min \sum_{i=1}^{n} x_i \\ &\text{s.t.} \quad 1.\ x_i \in \{0,1\}, \quad i = 1,\ldots,n \\ &\qquad 2.\ \text{structural requirements are satisfied} \end{aligned} \tag{1}$$

where n is the total number of possible locator locations, and x_i is a binary variable determining the presence (= 1) or absence (= 0) of a locator at its possible location. To avoid re-meshing of the panel during optimization, the possible locations of the locators are constrained to the nodal positions that will be on the perimeter of the frame upon the engagement.

Since the structure properties during the joint engagement are of interest, the locators are replaced with equivalent springs between the panel and the frame at the corresponding locations. The properties of the equivalent spring of a locator are obtained by measuring the tip deflections of the locator in response to the unit load in in-plane and out-of-plane directions using finite element analysis, as shown in Figure 5.

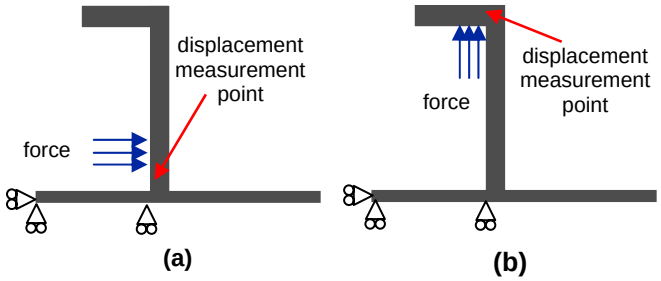

Figure 5: Measuring equivalent spring properties in (a) in-plane and (b) out-of-plane directions.

Snap Design

In order to realize unlocking upon heating, the snaps should be located in the region of the panel where all required

motion constraints are satisfied and the out-of-plane displacement larger than the snap height. Assuming the catch can be placed at an arbitrary location within the frame, the feasible region for potential snap placement is first selected by inspection, based on the motion constraints of the panel. Within the feasible region, the heating location with the minimum area is then obtained, such that the out-of-plane deflection is greater than the snap height. Finally, the snaps are simply placed at the location of maximum out-of-plane displacement within the feasible region.

The heating location is obtained by solving the following optimization problem:

$$\begin{aligned} &\min\ A(\boldsymbol{p}_1, \boldsymbol{p}_2, \boldsymbol{p}_3, \boldsymbol{p}_4) \\ &\text{s.t. } 1.\ \boldsymbol{p}_1, \boldsymbol{p}_2, \boldsymbol{p}_3, \boldsymbol{p}_4 \in F \\ &\quad 2.\ \boldsymbol{p}_1, \boldsymbol{p}_2, \boldsymbol{p}_3, \boldsymbol{p}_4 \text{ are distinct} \\ &\quad 3.\ \text{mininum out of plane displacement within } F > h \end{aligned} \tag{2}$$

where A is the area of the rectangular region on the panel defined by four vertices $\boldsymbol{p}_1$, $\boldsymbol{p}_2$, $\boldsymbol{p}_3$, and $\boldsymbol{p}_4$, F is the feasible region of snap placement on the panel, and h is the height of the snap (plus a small tolerance).

CASE STUDY

This section presents a case study on a simplified front fender panel of an automotive body shown in Figure 6. The size of the panel is approximately 600 mm by 1000 mm, with a thickness of 3 mm. The panel is assumed to be injection-molded from Nylon 66 with 30% glass, whose material properties are listed in Table 1. The frame is assumed as a hollow aluminum beam with a square cross section with 25 mm at external sides.

The optimization problem in the first step is solved using discrete genetic algorithms [25]. Because this step involves geometry, geometric crossover [26] and uniform crossover are used at 70% and 30%, respectively. On the other hand, the optimization problem in the second step is solved using real coded genetic algorithms [27]. The parameters used in GAs for this case study are shown in Table 2.

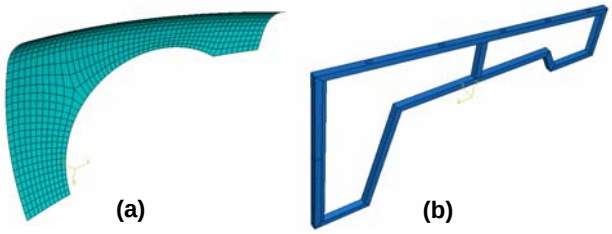

Figure 6: (a) simplified front fender panel and (b) internal frame.

Table 1: Material properties for Nylon 66 - 30% glass filled.

Property Name (units)	Value
Density (g/cm3)	1.36
Elasticity modulus (MPa)	8500
Poisson Ratio	0.36
Melting point (^{o}C)	260
Thermal expansion coefficient (m/m.^{o}C)	3.00
Specific heat capacity (j/kg.^{o}C)	1800
Conductivity (W/m.^{o}K)	0.40

Table 2: GA parameters used in this case study.

Parameter	Values for Step 1	Values for Step 2
Population size	150	60
Number of generations	50	40
Crossover probability	0.95	0.95
Mutation probability	0.05	0.05

Locator Design

Considering that the panel is injection-molded, the thicknesses of locators are kept the same as the panel thickness to avoid undesired defects such as sink mark on the external side. Figure 7 shows the dimensions of the locators, and Table 3 shows the properties of the equivalent spring for the locator, measured as shown in Figure 5.

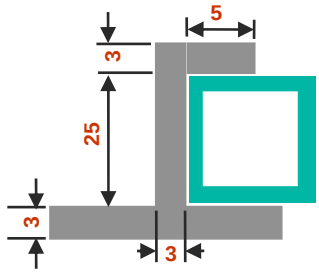

Figure 7: Locator dimensions for front fender panel.

Table 3: Properties of equivalent spring for the locator: in-plane stiffness (k_x) and out-of-plane plane stiffness (k_y).

k_x	4972.7 N/mm
k_y	5192.9 N/mm

The finite element model for the fender is shown in Figure 9. The nodes inside the thin rectangles represent the potential location of the locators. The numbers by the rectangles indicate the numbers of possible locator locations within the rectangles. The panel contains 123 possible locator locations (n = 123).

Automotive body panels are desired not to resonate at the frequencies of the vibrations occurring during the normal operation of the vehicle listed in Table 4 [28]. To avoid resonance at these frequency ranges, the locators must be

positioned such that the natural frequencies of the panel, when attached to the frame, do not fall within any of the listed ranges. The first 14 natural frequencies for the fender panels are checked against these constraints. To avoid the natural frequencies higher than the 14th from falling within the listed ranges, an extra constraint is added to the 14th natural frequency prohibiting it from being lower than 200 Hz. These constrains are treated as penalty terms added to the objective function in Equation (1). The modified objective functions are as follows.

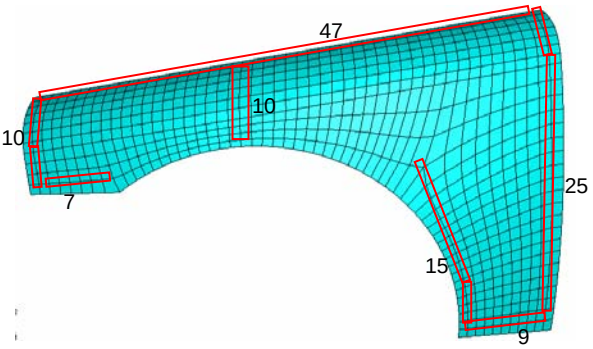

Figure 8: Finite element model for the fender. Nodes within the thin rectangles are the potential locations of locators

Table 4: Vehicle sources of vibrations and their frequency ranges.

Vibration source	Frequency range (Hz)
Suspension and wheels	5-10
Engine	11-17
Body	25-40
Driveline	50-150
Harshness	<200

$$f = \sum_{i=1}^{n} a_i + 100 \times \sum_{i=1}^{n-1} a_i a_{i+1} + Vib\_Pen \tag{3}$$

$$Vib\_Pen = \sum_{i=1}^{14} \begin{cases} \left(\left(\frac{17}{2}\right)^2 - \left(\frac{17}{2} - \omega_i\right)^2\right) + & \text{if } \omega<17\text{Hz} \\ \left(\left(\frac{15}{2}\right)^2 - \left(\frac{65}{2} - \omega_i\right)^2\right) + & \text{if } 25<\omega<40\text{Hz} \\ \left(\left(\frac{150}{2}\right)^2 - \left(\frac{250}{2} - \omega_i\right)^2\right) + & \text{if } 50<\omega<200\text{Hz} \\ 0 & \text{else where} \end{cases} + \left(\omega_{14} - 200\right)^2 / 10 \quad \text{if } \omega_{14}<200\text{Hz} \tag{4}$$

In order to avoid the overlap of neighboring locators during thermal deformation, it is not wise to allow the presence of locators at two or more successive locations. Accordingly, another constraint (term $\sum a_i a_{i+1}$) is added to the objective function. Since, this constraint can normally be of the same order of magnitude as the main objective function $\sum a_i$, a factor of 100 is multiplied enhance the effect of this constraint. Also, since the first two prohibited frequency ranges are too close to each other (only 1 Hz difference), and the very low frequencies (<5 Hz) should also be prohibited, they are all combined to a one wider prohibited range of < 17 Hz.

Figure 9 shows the optimum locations of the locators indicated by arrows, consisting of 19 locators distributed along all potential locations. The panel with the optimized locators does not violate any constraints in (4); in fact all the natural frequency values are higher than the highest prohibited natural frequency as shown in the second column of Table 5. For comparison, the first column of Table 5 shows the natural frequency values of the panel attached to the frame by bolted joints (*i.e.*, rigid connection) at the same location. It can be seen that the frequency values with locators are comparable to the ones with bolted joint, indicating the high rigidity of the proposed heat-reversible snaps joints. The mode shapes for the fender panel with locators are shown in appendix A.

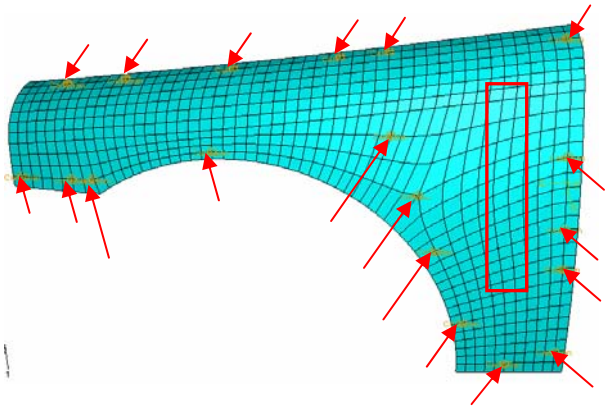

Figure 9: Optimum location of locators and feasible region for snap placement.

Table 5: Natural frequencies of the fender panel with optimum locators of locators (second column), and with bolted joints at the same location (third column)

Mode number	Frequency – locators (Hz)	Frequency – bolted (Hz)
1	201.43	225.08
2	206.96	226.66
3	210.77	237.25
4	213.76	244.72
5	224.56	272.24
6	248.60	282.43
7	265.65	296.22
8	274.21	308.02
9	280.72	334.28
10	300.46	343.71

Snap Design

The optimal heating locations are obtained by assuming h = 3 mm, and the heating temperature = 200 ^{o}C (below melting point 260 ^{o}C of the material). During heating, the rest of the panel is kept at 20 ^{o}C (Room temperature). The heat is assumed to be transferred to air through free (natural) convection only. The value of the convection heat transfer coefficient for air is chosen to be 8 W/m^2.^{o}K.

The optimal location of heating is also shown as a rectangle in Figure 9, with an area of 334 x 67 mm^2. The resulting temperature distribution and thermal deformations are shown in Figures 10 and 11, respectively. The maximum and minimum out-of-plane displacements (Δ_y) within the heated zone are 3.766 mm and 3.037 mm, respectively. Therefore, snaps that are 3 mm in height can be located at the center of the heated zone and guarantee opening. As shown in Figures 11 (c) and (d), the in-plane displacement (Δ_x and Δ_z), which might potentially interfere the smooth unlocking of the snap, is negligible compared to the out-of-plane displacement.

As seen in Figure 11 (a), the location of the maximum in-plane displacement coincides with the heating location, where the snaps (with less than 4 mm high) can be placed to realize the desired unlocking. Figure 12 (a) illustrates an example on how the snaps can be arranged, together with the locators. The locking plane of the snap is facing negative z-direction shown in Figure 12 (b), constraining the panel motion in the direction upon engagement.

Figure 13 shows a close-up view of a locator on the top edge of the panel in Figure 12 (a). The locators are to be fit into the slots cut on the frame. Using the L-shape, the locators on the top edge constrain the panel motion in positive z direction, and in both positive and negative x directions. Assuming the width of the slot in y direction on the frame are the same as the one of the locators, they also constrain the panel motion in both positive and negative y directions.

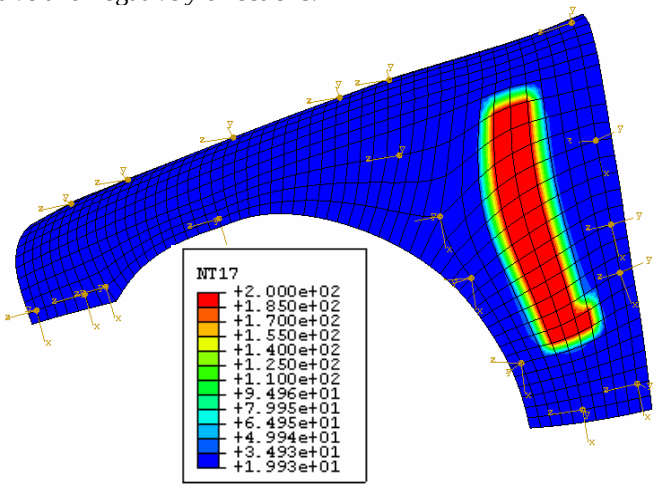

Figure 10: temperature distribution due to heating at the optimal location.

Figures 14 shows a close-up view of the cross sections of the locators and the frame at sections A-A and B-B in Figure 12 (a). The locator at A-A and the ones in the same orientation in Figure 12 (a) wrap around the frame to constrain the panel motion in positive z direction, and in both positive and negative y directions. Similarly, the locator at B-B and the ones in the same orientation in Figure 12 (a) constrain the panel motion in positive x direction, and in both positive and negative y directions.

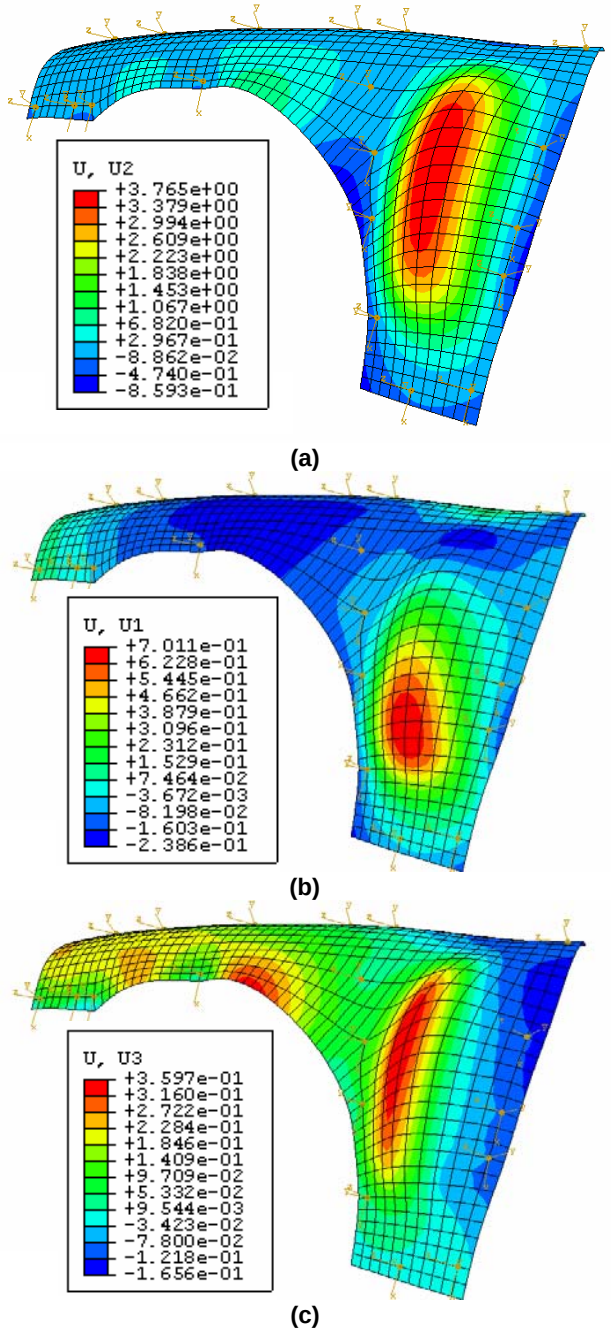

Figure 11: Thermal deformation (a) Deflection in y direction (out of plane), (b) deflection in x direction (in plane), and (c) deflection in z direction (in plane).

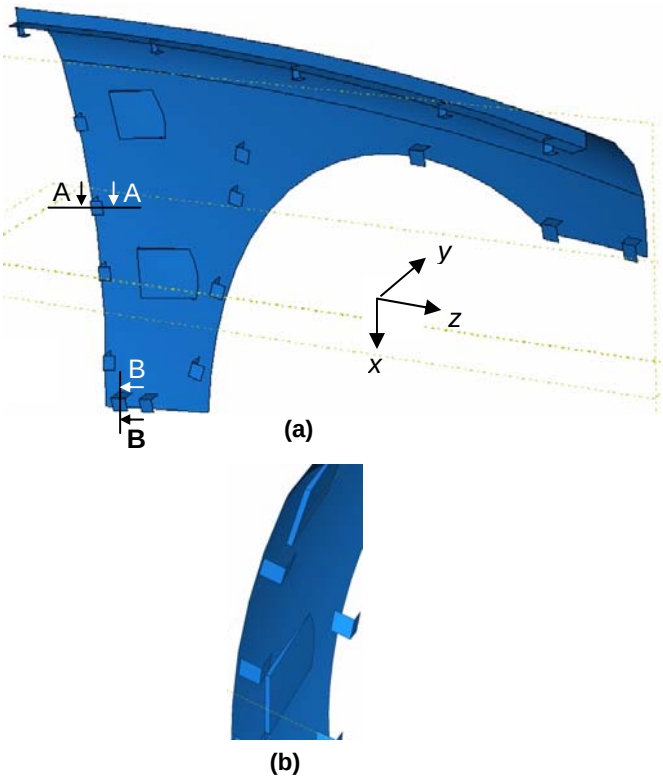

Figure 12: Panel with optimal locators and snaps: (a) Inside view of the entire panel and (b) close up view near A-A part looking in z-direction.

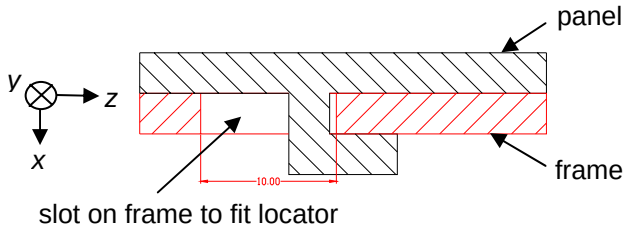

Figure 13: Close-up view of a locator on the top edge of the panel in Figure 12, viewing in positive y direction.

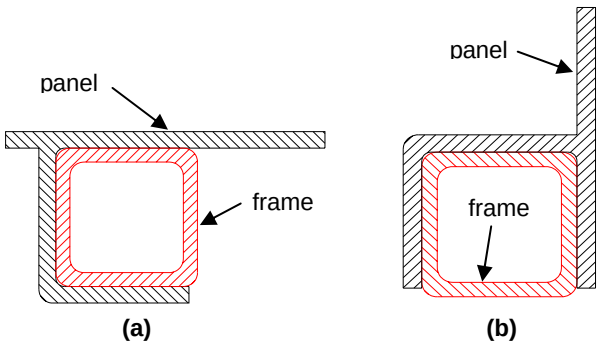

Figure 14: Close-up view of the cross sections of locator and frame: (a) section A-A and (b) section B-B.

From the orientation in Figure 12 (a), the panel can be attached to the frame of the same orientation (assumed stationary) as follows:

1. Push the panel to the frame (as in Figure 3 (a)) in negative *y* direction.
2. Slide the panel to the frame (as in Figure 3 (b)) first in positive *x* direction and then in positive *z* direction.

Upon unlocking of the snap with heating, the panel can be removed from the frame as follows:

1. Slide the panel on the frame (as in Figure 4 (c)) first in negative *z* direction, and then negative *x* direction.
2. Remove the panel from the frame (as in Figure 4 (c)) in positive *y* direction.

For proper constraining of the panel motion, of course, it is important that the tolerances of the locator dimensions are appropriately designed, so they fit with the frame (or slots on the frame) with interference or at least transition fit.

CONCLUSION AND FUTURE WORK

This paper presented the design of new joints, heat-reversible snaps, which allow easy, non-destructive, and clean detaching between internal frames and external panels in automotive bodies. It is expected to dramatically reduce the end-of-life environmental impacts of the aluminum space frame bodies, which currently suffer from poor material recyclability. While the assembly process is analogous to normal locator-snap systems, the heat-reversible snaps can be unlocked non-destructively upon heating the panel at a certain location, via the non-uniform thermal deformation of the panel. The optimum number and locations of the locators on the given panel were found based on the equivalent springs that represent the stiffness of the locator. Then, the snap and heating locations that ensure unlocking upon heating of the minimum area on the panel were obtained. A case study on an automotive fender panel assembly exhibited a promising result.

Actual automotive panels have much more complicated geometries than the simple panel model presented in this paper. As a future work, the method needs to be verified for more realistic panel geometries. The two-step approach may not work for complicated geometries due to the complex interaction between locator locations, heating locations, and the region of the maximum out-of-plane displacements. In such cases, a simultaneous optimization of locator, snap, heating locations are desired. This would require effective approximation models in each analysis domain, in order to overcome the increased computational time.

While developed for automotive panel/frame assembly, the design concept is generic and can be applied to different areas, where a clean separation is desired. The results will be reported in future publications.

ACKNOWLEDGMENTS

The authors gratefully acknowledge the funding provided by Toyota Motor Corporation, Japan, for this research.

REFERENCES

[1] Das, S., 2000, "Life-Cycle Impacts of Aluminum Body-in-White Automotive Material," The journal of the Minerals, Metals & Materials Society, **52**, pp. 41-44.

[2] "Design for aluminum recycling," 1993, Automotive Engineering, **101**, pp. 65-68.

[3] Audi Space Frame (ASF ®) aluminum body structure. http://www.audi.com

[4] Martchek, K., Fisher, E., Wasson, A., 1996, "A Response to "The Environmental Impact of Steel and Aluminum Body-in-Whites," The journal of the Minerals, Metals & Materials Society, **48**, pp. 40-41.

[5] Audi world, http://www.audiworld.com

[6] Shetty, D., Rawolle, K. and Campana, C., 2000, "A New Methodology for Ease-of-Disassembly in Product Design," Recent Advances in Design for Manufacture (DFM), **109**, pp. 39-50.

[7] Suri, G.. and Luscher, A., 1999, "Structural Abstraction in Snap-fit Analysis," *Proceedings of the 1999 ASME Design Engineering Technical Conferences*, Las Vegas, Nevada, September 12-15, DETC1999/DAC-8567.

[8] Nichols, D. and Luscher, A., 1999, "Generation of Design Data through Numerical Modeling of a Post and Dome Feature," *Proceedings of the 1999 ASME Design Engineering Technical Conferences*, Las Vegas, Nevada, September 12-15, DETC1999/DAC-8596.

[9] Turnbull, V., 1984, "Design Considerations for Cantilever Snap-Fit Latches in Thermoplastics," *Proceedings of the Winter Annual Meeting of ASME*, 84-WA/Mats-28, pp. 1-8.

[10] Wang, L., Gabriele, G. and Luscher, A., 1995, "Failure Analysis of a Bayonet-Finger Snap-Fit," *Proceedings of the ANTEC '95*, pp. 3799-3803.

[11] Larsen G. and Larson, R., 1994, "Parametric Finite-Element Analysis of U-Shaped Snap-Fits," *Proceedings of the ANTEC '94*, pp. 3081-3084.

[12] Genc, S., Messler, R., Bonenberger, P. and Gabriele, G., 1997, "Enumeration of Possible Design Options for Integral Attachment Using a Hierarchical Classification Scheme," *ASME Journal of Mechanical Design*, **119**, pp. 178-184.

[13] Genc, S. Messler Jr., R. and Gabriele, G., 1998, "A Systematic Approach to Integral Snap-Fit Attachment Design," Research in Engineering Design, **10**, pp. 84-93.

[14] Genc, S. Messler Jr., R. and Gabriele, G., 1998, "A Hierarchical Classification Scheme to Define and Order the Design Space for Integral Snap-Fit Assembly," Research in Engineering Design, **10**, pp. 94-106.

[15] Luscher, A., Suri G. and Bodmann, D., 1998, "Enumeration of Snap-Fit Assembly Motions," *Proceedings of ANTEC '98*, pp. 2677-2681.

[16] Chiodo, J., Billett, E. and Harrison D., 1999, "Preliminary Investigation of Active Disassembly Using Shape Memory Polymers," *Proceedings of the Eco-Design '99: First International Symposium on Environmentally Conscious Design and Inverse Manufacturing*, pp. 590-596.

[17] Chiodo, J., Billett, E. and Harrison, D., 1999, "Active Disassembly Using Shape Memory Polymers for the Mobile Industry," *IEEE International Symposium on Electronics and the Environment - ISEE – 1999*, Danvers, Massachusetts, May 11-13, pp. 151-156.

[18] Chiodo, J., McLaren, J., Billett, E. and Harrison, D., 2000, "Isolating LCD's at End-of-Life using Active Disassembly Technology: A Feasibility Study," *The proceedings of the IEEE International Symposium on Electronics and the Environment*, May 8-10, San Francisco, California, pp. 318-323.

[19] Chiodo, J., Jones, N., Billett, E. and Harrison, D., 2002, "Shape memory alloy actuators for active disassembly using 'smart' materials of consumer electronic products," Materials and Design, **23**, pp. 471-478.

[20] Masui K., Mizuhara, K. Ishii, K. and Rose, C., 1999, "Development of Products Embedded Disassembly Process Based on End-of-Life Strategies," *Proceedings of the EcoDesign '99: First International Symposium on Environmentally Conscious Design and Inverse Manufacturing*, pp. 570-575.

[21] Li, Y., Saitou, K., Kikuchi N., Skerlos, S., and Papalambros, P., 2001, "Design of Heat-Activated Reversible Integral Attachments for Product-Embedded Disassembly," *Proceedings of the EcoDesign 2001: 2nd International Symposium on Environmentally Conscious Design and Inverse Manufacturing*, Tokyo, Japan, December 12–15, p. 360–365.

[22] Li, Y., Saitou, K., and Kikuchi, N., 2003, "Design of Heat-Activated Reversible Integral Attachments for Product-Embedded Disassembly," International Journal of CAD/CAM, **3**, pp. 26-40.

[23] Li, Y., Saitou, K., Kikuchi N., 2002, "Design of Heat-Activated Compliant Mechanisms for Product-Embedded Disassembly," *Proceedings of the Fifth World Congress on Computational Mechanics*, Vienna, Austria, July 7-12.

[24] Bonenberger, Paul R., 2000, *The First Snap- fit Handbook, Creating Attachments for Plastic Parts*, Hanser Gardner Publication, Inc., Cincinnati.

[25] Goldberg, D., 1989, *Genetic Algorithms in Search, Optimization, and Machine Learning*, Addison-Wesley, Reading, Massachusetts.

[26] Pereira, F., Machado, P., Costa, E., and Cardoso, A., 1999, "Graph Based Crossover – A Case Study with the Busy Beaver Problem," *Proceedings of the 1999 Genetic and Evolutionary Computation Conference*.

[27] Michaelwicz, Z., 1996, *Genetic Algorithms + Data Structures = Evolution Programs*, 3rd Edition, Springer-Verlag, Berlin, Heidelberg.

[28] Kasravi, K. “vehicle body design,” TEC 452, Central Michigan University. www.kasravi.com/cmu/tec452/BodyEngineering/VibrationNoise.htm

APPENDIX A

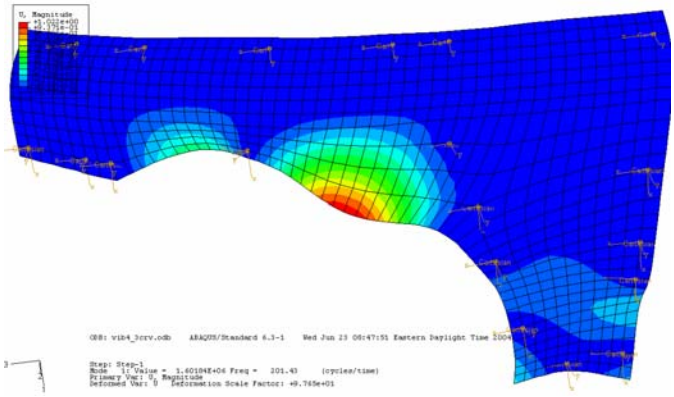

Figure A1: 1st mode shape ω_1 = 201.43 Hz

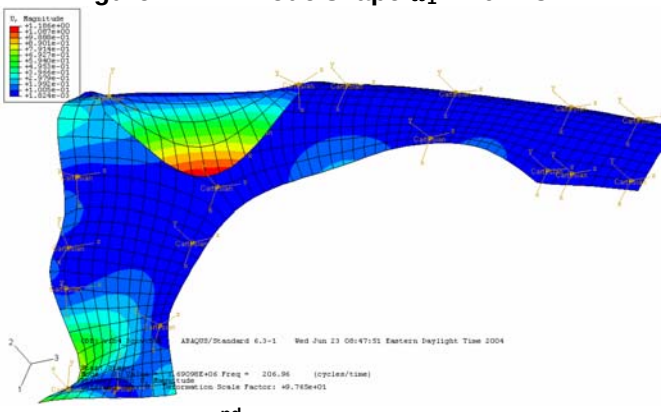

Figure A2: 2nd mode shape ω_2 = 206.96 Hz

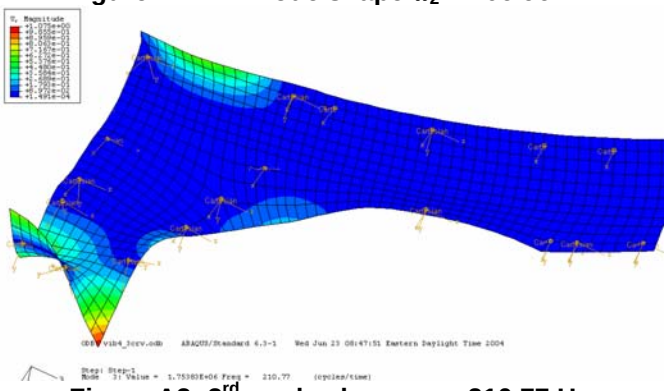

Figure A3: 3rd mode shape ω_3 = 210.77 Hz

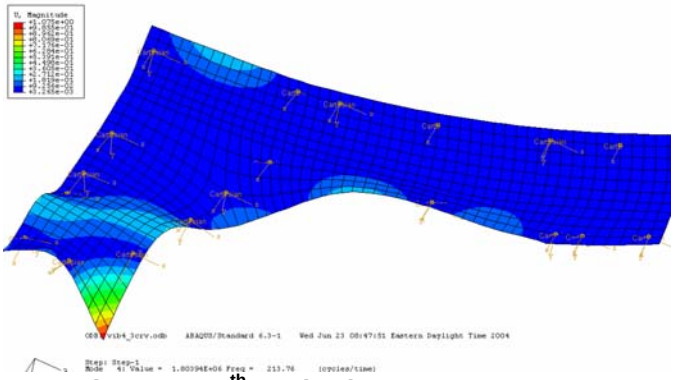

Figure A4: 4th mode shape ω_4 = 213.76 Hz

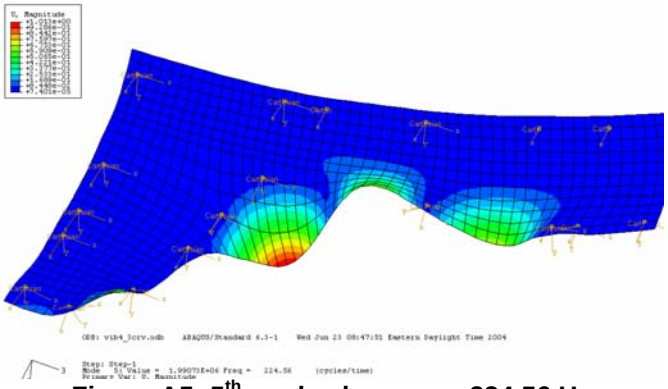

Figure A5: 5th mode shape ω_5 = 224.56 Hz

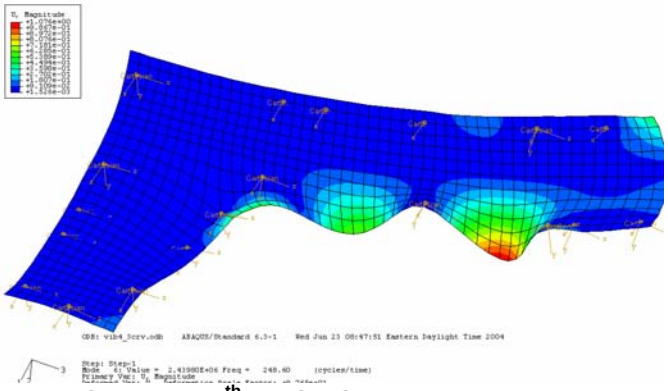

Figure A6: 6th mode shape ω_6 = 248.60 Hz

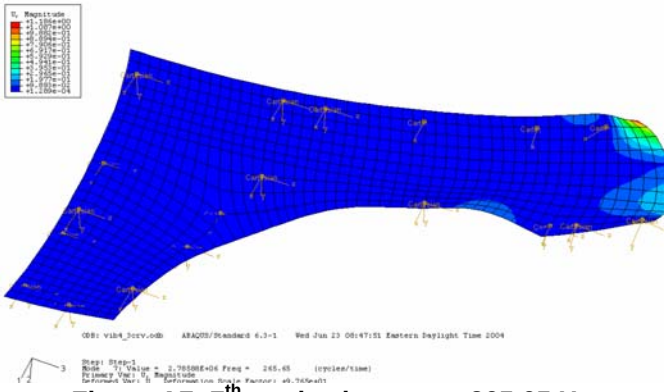

Figure A7: 7th mode shape ω_7 = 265.65 Hz

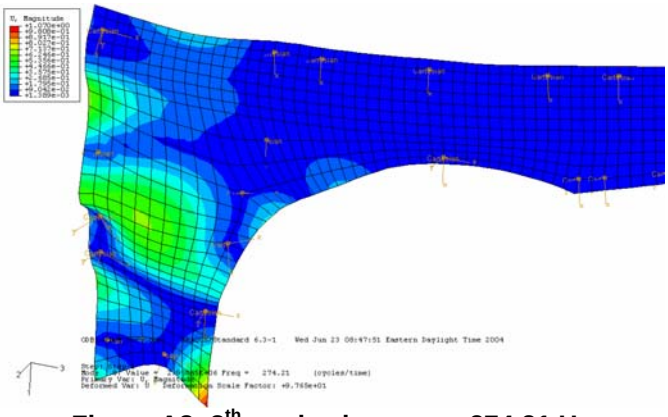

Figure A8: 8th mode shape ω_8 = 274.21 Hz

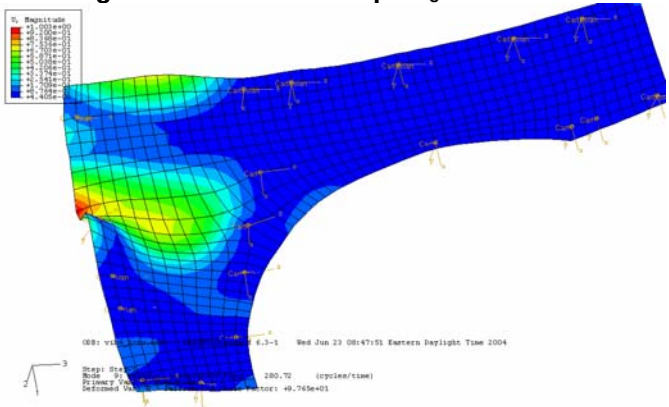

Figure A9: 9th mode shape ω_9 = 280.72 Hz

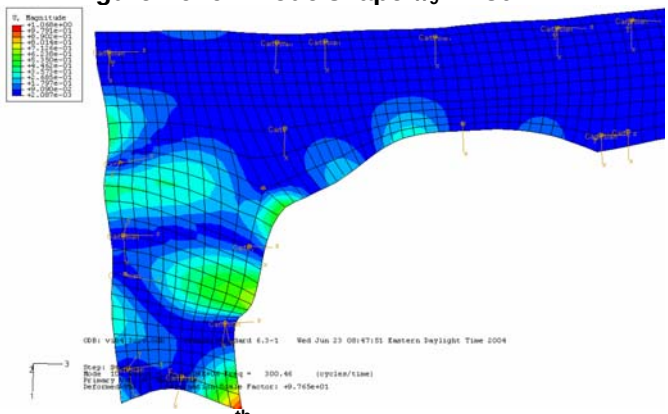

Figure A10: 10th mode shape ω_{10} = 300.46 Hz